



HAL
open science

Carbon nanotubes accelerate acetoclastic methanogenesis: From pure cultures to anaerobic soils

Leilei Xiao, Shiling Zheng, Eric Lichtfouse, Min Luo, Yang Tan, Fanghua Liu

► To cite this version:

Leilei Xiao, Shiling Zheng, Eric Lichtfouse, Min Luo, Yang Tan, et al.. Carbon nanotubes accelerate acetoclastic methanogenesis: From pure cultures to anaerobic soils. *Soil Biology and Biochemistry*, 2020, 150, 10.1016/j.soilbio.2020.107938 . hal-02930808

HAL Id: hal-02930808

<https://hal.science/hal-02930808>

Submitted on 4 Sep 2020

HAL is a multi-disciplinary open access archive for the deposit and dissemination of scientific research documents, whether they are published or not. The documents may come from teaching and research institutions in France or abroad, or from public or private research centers.

L'archive ouverte pluridisciplinaire **HAL**, est destinée au dépôt et à la diffusion de documents scientifiques de niveau recherche, publiés ou non, émanant des établissements d'enseignement et de recherche français ou étrangers, des laboratoires publics ou privés.

Carbon nanotubes accelerate acetoclastic methanogenesis: From pure cultures to anaerobic soils

Leilei Xiao^{a,e,f}, Shiling Zheng^{a,f}, Eric Lichtfouse^c, Min Luo^d, Yang Tan^f, Fanghua Liu^{a,b,e,f,*}

^a Key Laboratory of Coastal Biology and Biological Resources Utilization, Yantai Institute of Coastal Zone Research, Chinese Academy of Sciences, Yantai, 264003, PR China

^b Laboratory for Marine Biology and Biotechnology, Qingdao National Laboratory for Marine Science and Technology, Qingdao, 266237, PR China

^c Aix-Marseille Univ, CNRS, IRD, INRAE, Coll France, CEREGE, Avenue Louis Philibert, Aix en Provence, 13100, France

^d School of Environment and Resource, Fuzhou University, Fuzhou, 350116, PR China

^e Center for Ocean Mega-Science, Chinese Academy of Sciences, Qingdao, 266071, PR China

^f CAS Key Laboratory of Coastal Environmental Processes and Ecological Remediation, Yantai Institute of Coastal Zone Research (YIC), Chinese Academy of Sciences (CAS), Yantai, Shandong, 264003, PR China

ARTICLE INFO

Keywords:

Methane
DIET-independent methanogenesis
Conductive material
Acetoclastic methanogenesis
Pure culture
Proteome

ABSTRACT

Direct interspecies electron transfer (DIET) between electricigens and methanogens has been shown to favour CO₂ reduction to produce biomethane. Furthermore, DIET is accelerated by conductive materials. However, whether conductive materials can promote other methanogenic pathways is unclear due to a lack of detailed experimental data and the poor mechanistic studies. Here, we hypothesized that conductive carbon nanotubes (CNTs) stimulate acetoclastic methanogenesis independently of electricigens in pure cultures of *Methanosarcina* spp. and anaerobic wetland soil. We found a significant increase in the methane production rate during the growth phase, e.g. from 0.169 mM to 0.241 mM after addition of CNTs on the 3rd day. CNTs did not increase the abundance of electromicroorganisms or the electron transfer rate in anaerobic soils, using via microbial diversity and electrochemical analysis. ¹³C-CH₃COOH labelling, stable carbon isotope fractionation and the CH₃F inhibitor of acetoclastic methanogenesis were used to distinguish methanogenic pathways. CNTs mainly accelerated acetoclastic methanogenesis rather than CO₂ reduction in both pure cultures and anaerobic soils. Furthermore, the presence of CNTs slightly alleviate the inhibition of CH₃F on acetoclastic methanogenesis during the pure culture of *Methanosarcina barkeri* and *Methanosarcina mazei* with the production of more than 0.3 mM methane. CNTs closely attached to the cell surface were observed by transmission electron microscopy. Proteome analysis revealed a stimulation of protein synthesis with about twice the improvement involved in -COOH oxidation and electron transfer. Overall, our findings demonstrate that conducting CNTs favor methane production and that the mechanism involved is acetoclastic methanogenesis via acetate dismutation, at least partly, rather than classical CO₂ reduction.

1. Introduction

Methane plays a crucial role globally as a greenhouse gas and a source of renewable fuel. Biomethane is typically produced by the cooperation of various microorganisms such as fermenting microorganisms and methanogenic archaea or methanogens (Liu et al., 2018; Zhu et al., 2018). Fermenting microorganisms are responsible for producing methanogenic substrates, such as acetate and CO₂. Methanogens produce methane as the end-product of their anaerobic respiration to obtain energy. The common habitats of methanogens include sediments,

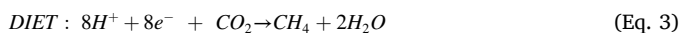
anaerobic soils, landfills and so on (Ji et al., 2018; Xiao et al., 2019a). 77.4% of the cultivated methanogens can reduce CO₂, and the next most abundant type of metabolism is methylotrophic methanogenesis (Holmes and Smith, 2016). The acetoclastic methanogenic pathway is by far the least metabolism, only 12 species in two genera, namely, *Methanosarcina* and *Methanosaeta* (formerly known as *Methanothrix*), able to utilize acetate as a carbon and energy source (Holmes and Smith, 2016). *Methanosarcina* is a metabolically versatile methanogen with the ability to use CO₂, acetate and methyl compounds to generate methane (Rother and Metcalf, 2004). For example, research published 40 years

* Corresponding author. Yantai Institute of Coastal Zone Research, 17 Chunhui Road, Laishan District, Yantai, Shandong, 264003, China.

E-mail address: fhliu@yic.ac.cn (F. Liu).

ago has confirmed acetate, methanol and CO₂ as substrates for growth of *Methanosarcina barkeri* (Hutten et al., 1980).

Methylotrophic methanogenesis contributes a very small amount of methane accumulation (Conrad, 2005). Therefore, two other pathways mainly account for biomethane production: acetoclastic methanogenesis (Eq. (1)) and CO₂ reduction, which contribute to approximately 2/3 and 1/3 of the global biomethane production, respectively (Conrad, 2005). CO₂ reduction is performed either by hydrogenotrophic methanogenesis (Eq. (2)) or direct interspecies electron transfer (DIET, Eq. (3)).



During acetoclastic methanogenesis, methanogenic archaea convert acetate into methane and CO₂ by dismutation (Eq. (1)). Here, the acetate carboxyl group is oxidized to CO₂ with the release of electrons (Li et al., 2006). Then, electrons are used to reduce CoM-S-S-CoB that transforms the acetate methyl to form methane. As a consequence, a complete acetoclastic methanogenesis has no net electron gains or losses. During hydrogenotrophic methanogenesis, CO₂ is reduced by H₂ (Eq. (2)). Specifically, CO₂ is first reduced to methanofuran-CHO, and then, a series of intermediate metabolites are involved such as methyl-tetrahydromethanopterin-HCO and methyl-tetrahydromethanopterin-CH₃ (H₄MPT-CH₃). From H₄MPT-CH₃ to methane, hydrogenotrophic methanogenesis and acetoclastic methanogenesis share the same route. DIET coupling exoelectrogenic bacteria and methanogens has been further proposed to explain methanogenesis in complex environments (Morita et al., 2011; Song et al., 2019; Xiao et al., 2019a,c). This coupling can be strengthened by the addition of conductive materials (Liu et al., 2012; Lu et al., 2020; Viggli et al., 2014; Xiao et al., 2018; Xiao et al., 2019b).

DIET coupled to CO₂ reduction is the main mechanism referred to explain methane production. Nonetheless, this has been unequivocally demonstrated only in cocultures of *Geobacter* with *Methanosaeta* or *Methanosarcina* (Martins et al., 2018; Van Steendam et al., 2019). Interestingly, it is acetotrophic methanogens rather than hydrogenotrophic methanogens that can accept electrons to reduce CO₂. Insights into an alternative mechanism come from enhanced acetate dismutation by conductive materials (Fu et al., 2019; Li et al., 2018). For instance, Fu et al. (2019) disclosed that nano-Fe₃O₄ acted as an intracellular electron shuttle to accelerate acetoclastic methanogenesis by culturing *M. barkeri* with acetate as a carbon source. Whereas, redox cycling of Fe (II) and Fe (III) in nano-magnetite in the extracellular space accelerated acetoclastic methanogenesis by cultivating *Methanosarcina mazei* (Wang et al., 2020). These studies evidence the acceleration of acetate dismutation. However, the mechanism of increased acetoclastic methanogenesis is still poorly understood. Concerning iron ions may be used as nutrients to improve the activity and function of methanogens. Therefore, more work is needed to verify the benefits from conductivity. As human activities increase, more and more carbon nanomaterials end up into soils (Rai et al., 2018; Usman et al., 2020). Nano-magnetite has been found to accelerate methane production by acetate dismutation in pure culture. However, it is still unclear how conductive nanomaterials work to accelerate acetoclastic methanogenesis in multicommunity environments.

To accurately distinguish the source of methane, multiple techniques are necessary. CH₃F is an inhibitor of acetoclastic methanogenesis, which is widely used to analyze the contribution of CO₂ reduction and acetate dismutation (Conrad and Casper, 2010; Ji et al., 2018; Xiao et al., 2018). In brief, methane accumulation comes from both CO₂ reduction and acetoclastic methanogenesis without CH₃F. Whereas only CO₂ reduction can contribute to methane production in the presence of CH₃F. The difference between the two treatments thus reveals the contribution of acetoclastic methanogenesis. In addition to the use of

CH₃F, stable isotope fractionation is a more precise and accurate method (Conrad, 2005). Although these methods are widely used to distinguish traditional methane production pathways, these methods are rarely used to study methane production influenced by electromicroorganisms and conductive materials (Xiao et al., 2020).

Here, we propose an alternative mechanism of acetoclastic methanogenesis involving electron transfer by conductive carbon materials and we explain the mechanism in depth. To test this hypothesis we studied methane production in pure cultures of *M. barkeri*, *M. mazei* and in anaerobic soil containing carbon nanotubes (CNTs). The mechanisms were qualitatively and quantitatively assessed by ¹³C tracing, CH₃F methanogenic inhibition, proteome analysis, thermodynamic analysis, electrochemical analysis, modelling and microscopy.

2. Materials and methods

2.1. Microorganisms and growth conditions for pure culture

Experiment 1: Mineral salt medium, as described elsewhere (Zehnder and Wuhmann, 1977), was used to culture *M. barkeri* and *M. mazei* under strict anaerobic conditions with ~20 mmol L⁻¹ acetate as the methanogenic substrate. In addition to H₂, some components with reducibility, such as cysteine and Na₂S, may act as electron donors to reduce CO₂ to produce methane. In this study, the final concentration of cysteine was about 1 mM, and it was approximately 0.5 mM for Na₂S. Therefore, two kinds of methanogenic substrates were provided including acetate and CO₂. Anaerobic tubes (25 mL total volume, medium volume of 10 mL) were pressurized with a mixture of N₂/CO₂ (80%/20%). All incubations were conducted at 30 °C in the dark. In this study, carbon nanotubes were purchased from Macklin (Shanghai, China; CAS: 308068-56-6, Lot#:C10112635, Inner diameter: 5–10 nm, Outer diameter: 10–20 nm, Length: 500–2000 nm). No nanotubes was added in the control group, and the experimental group was added artificially. The final concentration of CNTs was ~0.2 g/L. According to visual observation, most of the CNTs were deposited on the bottom of the vials. The concentration of produced gases was tested using a gas chromatograph (GC; Agilent 7820A, USA) equipped with a flame ionization detector (FID) and a thermal conductivity detector (TCD). A possible dissolution of methane in the medium can be neglected as follows: in the vials with a headspace-to-medium ratio of 15 mL/10 mL, the percentage of methane in the gas phase (f_g) is 97.9% at 30 °C is given by

the equation $f_g = 100\% \cdot \frac{1}{K_H RT} \cdot \frac{V_g}{\frac{1}{K_H RT} \cdot \frac{V_g}{V_w} + 1}$ (Stumm and Morgan, 1996),

where V_g and V_w are the volumes of the gaseous and aqueous phases, respectively, R is the ideal gas constant, and a value of 0.0013 mol L⁻¹ atm⁻¹ is used for Henry's law constant, K_H. The column is a Hayesep Q 80–100 mesh (6 ft × 1.8" × 2.0 mm). High-pressure liquid chromatography (HPLC; Agilent 1260 Infinity) was used to test the acetate concentration.

Experiment 2: CH₃F, an inhibitor of acetoclastic methanogenesis (Conrad, 2005), was applied to explore whether CNTs can improve the ability of *M. barkeri* to endure hostile environments. CH₃F was applied at 1.5% v/v to replace the equal gas mixture (N₂/CO₂, 80%/20%) in the vials, other operations can refer to experiment 1.

2.2. Analysis of potential methane production pathways in pure culture systems with ¹³C labelling

Experiment 3: To clarify the methanogenic pathways for methane accumulation with and without CH₃F, carbon isotopes of CH₄ (¹³CH₄/¹²CH₄) were tested. CH₄ collected from the headspace was tested to obtain the δ¹³C value using a gas chromatograph combustion isotope ratio mass spectrometer (GC–C–IRMS) system (Thermo Fisher MAT253, Germany). To eliminate the interference of original CO₂, separation of CH₄/CO₂ was performed in a Finnigan Precon. In brief, mixed gas (~1 mL) was injected into a sample container (100 mL),

which was filled with helium gas (99.999% purity) beforehand. Helium loaded the mixture into a chemical trap, which can be applied to scrub CO₂ and H₂O. Then, CH₄ can be oxidized in a combustion reactor at 960 °C and converted to CO₂ and water. After that, the combusted CO₂ was subsequently purified by two liquid nitrogen cold traps with internal filling of Ni wires and then transferred into the IRMS for determination. The precision of repeated analyses was ±0.2‰ when 1.3 nmol methane was injected. The abundance of ¹³C in a sample is given relative to a standard using the δ notation:

$$\delta^{13}\text{C} = \left[\left(\frac{{}^{13}\text{C}}{{}^{12}\text{C}} \right)_{\text{sample}} / \left(\frac{{}^{13}\text{C}}{{}^{12}\text{C}} \right)_{\text{PDB}} - 1 \right] \times 1000.$$

where PDB refers to the Pee Dee Belemnite carbonate that is used as standard which has a ¹³C/¹²C ratio of 0.0112372.

Experiment 4: To test methane production pathway of *M. barkeri* and *M. mazei* in the presence of CH₃F. Artificial abundance of ¹³CH₃COOH (3% and 5%) was used in pure culture. The test of ¹³CH₄/¹²CH₄ was performed as described in Experiment 3.

2.3. LC-MS/MS based methanogen proteomics

Experiment 5: Proteome analysis was used to determine how CNTs increased the competitiveness of the acetoclastic methanogenic pathway. *M. barkeri* cells were obtained following the operation of Experiment 1 and proteins of this archaea were analyzed by LC-MS/MS. Three replicates were conducted. Briefly, the total protein collected from each sample, sampled on the 25th day, was digested with trypsin and then the peptides were labelled using a 6-plex TMT reagent Multiplex kit (Applied Biosystems, Foster City, CA) according to the manufacturer's protocol. A Triple TOF 6600 mass spectrometer (SCIEX, Concord, Ontario, Canada) was used to acquire the data. Based on PCA analysis of proteome data (Fig. S1), one of the repeats of the CNT group was not considered in the subsequent analysis. The detailed methods regarding protein extraction and digestion, TMT labelling, and LC-MS/MS analysis can be found in the supporting information.

2.4. Microcosm cultivation and chemical analysis

Experiment 6: After intermittent flooding in October 2017, we sampled soil from the Yellow River Delta, which is a sensitive wetland with serious human intervention (Xiao et al., 2017). To prepare the slurry for the subsequent culture experiment, 150 g soils, 1.5 g dry ground straw of *Phragmites australis*, and 450 mL sterile water were added into a serum bottle with the total volume of 1000 mL. The detailed operation can be found in the supplementary materials. For the following experiments, vials with a volume of 11 mL were used to test the effect of CNTs on methane production in anaerobic soil. Three cycles of vacuum/charging high-purity N₂ were conducted to create anaerobic vials. Then, 5 mL portions of the slurry were dispensed into each vial. Suspensions of 10 g/L CNTs in ultrapure water were N₂ flushed and then sterilized. For treatment with CNTs, a CNT suspension (100 μL) was added to each vial to reach a concentration of about 0.2 g/L. An equal amount of water was added to the vial of the control group. A 400 μL acetate solution (0.275 M) was used as the substrate for methanogens with the final acetate concentration of approximately 20 mM. Overall, all treatments contained the same amount of upper space and slurry plus sterile water approximately 5.5 mL. Vials were sacrificed in triplicate to test the concentrations of acetate, methane, H₂ and CO₂ after a certain incubation period. A modified Gompertz model was used to quantitatively analyze the production of methane with and without CNTs in anaerobic soils:

$$P = P_{\max} * \exp \left\{ - \exp \left[\frac{R_{\max} * e}{P_{\max}} * (\lambda - t) + 1 \right] \right\}$$

where P is the methane concentration (mM) at time t, P_{max} is the

maximum methane concentration (mM), t is the time (D), R_{max} is the maximum methane production rate (mM D⁻¹), λ is the lag phase (D), and e is 2.71828. The kinetic parameters of biomethane production are shown in Table S2.

CH₃F was applied to inhibit the progress of direct acetate dismutation in anaerobic soil (Experiment 7). In addition to replacing the same amount of nitrogen with 1.5% CH₃F gas, other operations can refer to experiment 6.

Experiment 8: In addition to using the methanogenic inhibitor to analyze the respective contribution of acetoclastic methanogenesis to total methane production, carbon stable isotope fractionation and the related calculations were conducted. Gases collected from the headspace were used to test the δ¹³C-values of methane and CO₂. The test of the δ¹³C-values of methane can refer to Experiment 3. A similar method was used to test δ¹³C-values of CO₂. The chemical trap was replaced by a water trap. The α value can be calculated using the equation: α = $\frac{\delta^{13}\text{CO}_2 + 1000}{\delta^{13}\text{CH}_4 + 1000}$. For the calculation of f_{ma}, the equation was used as follows, $f_{ma} = \frac{\delta_{mc} - \delta^{13}\text{CH}_4}{\delta_{mc} - \delta_{ma}}$.

2.5. Calculation of Gibbs free energy for hydrogenotrophic and acetoclastic methanogenesis

Experiment 9: The Gibbs free energy (ΔG) of hydrogenotrophic methanogenesis was calculated based on the concentrations of H₂, CO₂ and CH₄ to analyze the potential contribution of different methanogenic pathways (Xiao et al., 2019b). Briefly, the following equation was used:

$$\Delta G = \Delta G^0 + RT * \left\{ \ln \left[\frac{C_{\text{CH}_4}}{(C_{\text{CO}_2} * C_{\text{H}_2}^4)} \right] \right\}$$

with ΔG⁰, ΔG at 273.15 K and 101.325 kPa; R, the ideal gas constant, 8.3145 J mol⁻¹·K⁻¹; T, the absolute thermodynamic temperature, 303.15 K; C_{CH₄}, C_{CO₂} and C_{H₂}: concentrations of methane, CO₂, and H₂, mol·L⁻¹. For the calculation of ΔG⁰, ΔG⁰ = ΔG_f⁰ - ΔS*(T_f-T₀), ΔG_f⁰, ΔG under 298.15 K and 101.325 kPa; ΔS, entropy change at 298.15 K; T_f and T₀, 298.15 K and 273.15 K, respectively. ΔG_f⁰ = ΔH-T_f*ΔS, ΔH, enthalpy change at 298.15 K.

For the calculation of ΔG of acetoclastic methanogenesis, the following equation holds:

$$\Delta G = \Delta G^0 + RT * \left\{ \ln \left[\frac{C_{\text{CH}_4} * C_{\text{CO}_2}}{(C_{\text{acetate}})} \right] \right\} + 2.303 * RT * N_{pH}$$

The definitions of the parameters are given above, except C_{acetate}, the acetate concentration, mol·L⁻¹ and N_{pH}, the pH value of the supernatant.

2.6. 16S rRNA gene sequencing

Experiment 10: Bacterial (Bac515F and Bac926R) and archaeal (Arch519F and Arch915R) primers were used to perform amplification of the 16S rRNA gene. After six days of incubation, the anaerobic soil samples were collected for microbial diversity determination. Three repetitions were carried out. An Illumina Miseq platform was used for sequencing after the construction of the amplicon library. The OTU taxonomies (from phylum to species) were determined based on the NCBI database. The raw sequencing reads have been deposited in the NCBI SRA (accession numbers SRP151406 and SRP151407 for bacteria and archaea, respectively).

2.7. Statistical analysis

Data are presented as the mean ± standard deviation of triplicate cultures. All statistical analyses were performed using Origin 2016 (Origin Lab Corporation, USA) software. A t-test was used to analyze the significance level, and a p value of less than 0.05 was considered

statistically significant.

3. Results

3.1. Effects of carbon nanotubes on methane production in pure cultures

We performed pure cultures of *Methanosarcina* species to test whether CNTs could promote methane production via acetoclastic methanogenesis. Acetate consumption and methane production were accelerated by CNTs for both species (Fig. 1a and b). However, CNTs showed no significant stimulation of the hydrogenotrophic methanogen *M. formicicum* (Fig. 1d). The absolute $\delta^{13}\text{C}$ values of the produced methane ranged from $-40.07 \pm 0.90\text{‰}$ to $-36.46 \pm 0.66\text{‰}$ for *M. barkeri* and from $-42.11 \pm 0.93\text{‰}$ to $-34.08 \pm 0.40\text{‰}$ for *M. mazei* (Fig. 1c). These values were in the range of that reported for acetoclastic methanogenesis in pure of *Methanosaeta concilii*, of -30 to -40‰ (Penning et al., 2006), thus supporting the occurrence of this pathway.

The $\delta^{13}\text{C}$ differences between the control and CNTs provided several insights. First, they indicated the existence of at least two mechanisms, namely, CO_2 reduction and acetate dismutation, since different mechanisms usually have different ^{13}C fractionation. Second, the highest $\delta^{13}\text{C}$ values of -34.08‰ and -36.46‰ observed with CNTs implied that CNTs favoured acetate dismutation because CO_2 reduction is expected to fractionate more and yield the more negative values (Conrad, 2005). We further compared the amount of methane produced in the experiments and theoretical calculations for acetate dismutation (Fig. S2). Calculations were consistent with experimental data for CNTs but differed in the control assay. These findings revealed a contribution of acetate dismutation with CNTs. We also performed incubations with the hydrogenotrophic methanogen *M. formicicum* to check whether the acceleration of methane production was due to CNT chemical reactivity (Fig. 1d). The results showed the absence of acetate consumption and methane production, thus disclosing the CNTs cannot independently accelerate acetate dismutation. Overall, acetoclastic methanogenesis may be the mechanism explaining methane production with CNTs.

To strengthen the acetoclastic methanogenesis hypothesis we performed incubations of *M. barkeri* with CH_3F and ^{13}C -labelled acetate

(Fig. 2). Without CNTs, CH_3F inhibited methanogenesis, as expected, as shown by the dotted green and orange bottom lines in Fig. 2a. This inhibition in the control assay was also confirmed by the low ^{13}C - CH_4 abundance below 1.118%, typical of natural abundance, in the presence of highly ^{13}C -labelled acetate (Fig. 2b). The minor methane production observed after 10 days was likely to be due to CO_2 reduction. By sharp contrast, the addition of CNTs induced a rapid increase in methane emission after 6 days in the presence of CH_3F , as shown by the solid green and orange lines down in Fig. 2a, and the emitted methane was highly ^{13}C -labelled (Fig. 2b). During the incubation of *M. barkeri* with the addition of CNTs, however, the methane produced in the presence of CH_3F (Fig. 2a) was only approximately 3% of that in the absence of CH_3F (Fig. 1b), and the acetate was hardly consumed during the whole incubation with the addition of CH_3F (Fig. 2b). Thus, CNTs could only slightly relieve the inhibition of acetate dismutation. Since this is a pure culture, interspecies electron transfer can be ruled out. These findings indicated the benefits of CNTs on methane production without the need for other electricigen species by promoting direct acetate dismutation (Eq. (1)).

M. barkeri and *M. mazei* produced methane through unexclusive acetoclastic methanogenesis even though 20 mM acetate was used as the substrate. Otherwise, the $\delta^{13}\text{C}$ - CH_4 should be the same, and the values may be even lower than -30‰ (Penning et al., 2006). Supplemental to a previous study (Salvador et al., 2017; Wang et al., 2020), CO_2 reduction may be involved in methane accumulation even though the substrate of *M. barkeri* and *M. mazei* was a high concentration of acetate.

3.2. Proteome analysis

We analyzed the proteome of *M. barkeri* cultivated with and without CNTs to obtain information on the effect of CNTs on protein expression resulting in an increase in acetoclastic methanogenesis. The abundance of proteins that may be involved in acetoclastic methanogenesis is given in Table S1. The regulation of the expression of proteins and enzymes was modified by the addition of CNTs (Fig. 3). For instance, the enzymes/proteins that control the oxidation of carboxyl groups, such as Ack and Codh-Acs, were highly up-regulated by 1.06 and 1.29 (orange

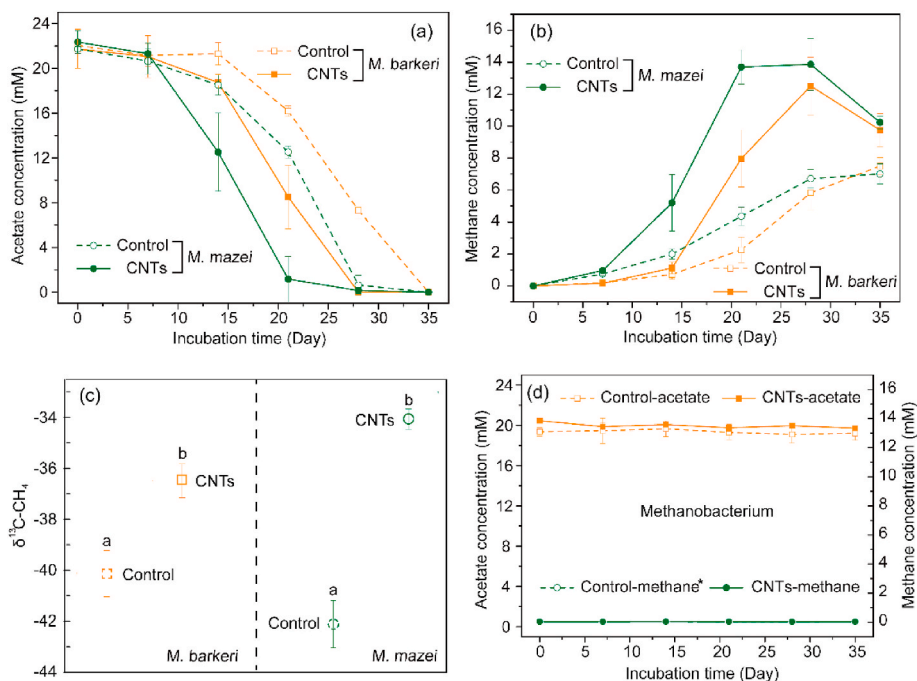


Fig. 1. Methanogenesis in pure cultures of *Methanosarcina* species on acetate substrate with carbon nanotubes (CNTs). a) Acetate concentration for *M. barkeri* and *M. mazei*. b) Methane production for *M. barkeri* and *M. mazei*. c) $\delta^{13}\text{C}$ in ‰ of CH_4 produced by *M. barkeri* and *M. mazei*. d) Acetate and methane concentrations in pure cultures of *M. formicicum*; note that the methane control gives similar data as the CNT assay.

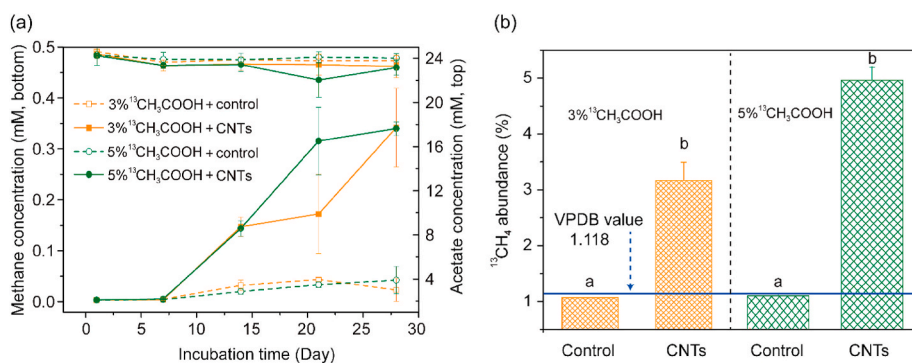


Fig. 2. Concentration and ^{13}C abundance of produced methane under artificial abundance of $^{13}\text{C}_3\text{COOH}$ with the presence of CH_3F for all treatments. 3% and 5% are ^{13}C versus ^{12}C for the Methyl C. Methane production and acetate consumption by *M. barkeri* under the conditions with CH_3F (a). The bottom four lines are the values of methane concentrations, and the top four lines was the values of acetate concentrations. The ^{13}C abundance of produced methane (b), which were compared with VPDB (Vienna Pee Dee belemnite).

arrows), thus showing that CNTs favoured acetoclastic methanogenesis. Moreover, the expression of ferredoxin (Fd) was highly increased by 1.62 and 1.69 for the two subunits of ferredoxin. By contrast, CNTs decreased the expression of proteins involved in methyl reduction, such as *mcrB*, and energy production, such as *atpB*. These results indicate the bypass of the classical cycle by CNTs. Overall, CNTs had some impact on the expression of proteins involved in acetoclastic methanogenesis, and suggest that CNTs may strengthen carboxyl oxidation and electron transfer.

3.3. Methane production in anaerobic soils amended with carbon nanotubes

We tested whether CNTs enhanced acetoclastic methanogenesis in complex microbial communities of anaerobic soils. The P_{max} (maximum methane concentration) values of the control and CNT treatments were 0.297 ± 0.016 and 0.304 ± 0.011 mM, respectively. The lag phase of methane production (λ) was approximately 0.6 days in the vials without CNTs. In the presence of CNTs, λ decreased by approximately 28.3%, with a value of ~ 0.43 days. Furthermore, CNTs promoted methane production, resulting in an increase in R_{max} with a value of 0.102 ± 0.010 mM D^{-1} compared to the control (0.087 ± 0.014 mM D^{-1}).

For the kinetics of ΔG of these two pathways, values were always negative, suggesting that producing methane with acetate or CO_2 as a substrate was feasible (Fig. 4b). The proportion of methane produced by the acetoclastic methanogenic pathway in total methane production remained relatively stable in the range of $\sim 60\%$ – $\sim 80\%$ for both treatments (Fig. 4c). Direct acetate dismutation contributed more to the net accumulation of methane than did CO_2 reduction (Fig. 4d). The proportion of this pathway reached its peak on the 3rd day. According to the results shown in Fig. 4e, methane yield occurred primarily due to enhancement of acetoclastic methanogenesis in anaerobic soil.

3.4. Impact of carbon nanotubes on carbon isotopic fractionation

Methane was mainly derived from the reduction of CO_2 in the case of the inhibition of acetoclastic methanogenesis, based on isotope results (Table 1). Combining the equations of hydrogenotrophic methanogenesis (Eq. (2)) and isotope fractionation of this reaction ($\alpha_{\text{CO}_2/\text{CH}_4} = \frac{\delta^{13}\text{C}_{\text{CO}_2} + 1000}{\delta^{13}\text{C}_{\text{CH}_4}(\text{CO}_2) + 1000}$), both treatments held the same α value (~ 1.05). δ_{mC} , which is the $\delta^{13}\text{C}$ value of methane from CO_2 reduction, was not influenced by CNTs. In contrast, CNTs changed the value of δ_{mA} ($p < 0.05$), which is the $\delta^{13}\text{C}$ value of methane from acetoclastic methanogenesis.

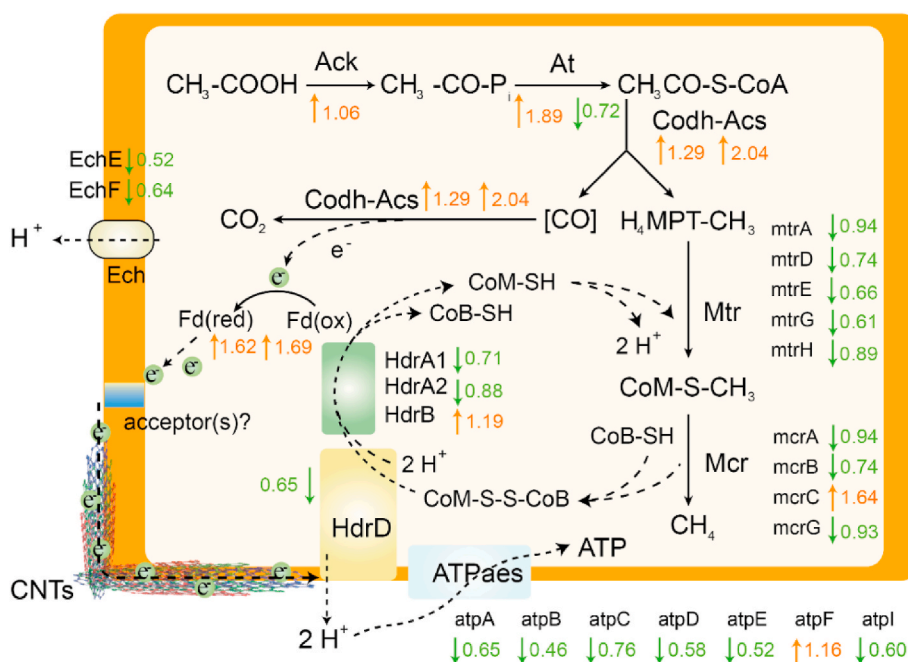


Fig. 3. Effect of carbon nanotubes (CNTs) on the expression of proteins and enzymes involved in acetoclastic methanogenesis. Up-regulation ratios (orange arrows) and down regulation ratios (green arrows) were determined by proteome analysis of pure cultures of *M. barkeri* with and without CNTs. The orange border represents a cell membrane. (For interpretation of the references to colour in this figure legend, the reader is referred to the Web version of this article.)

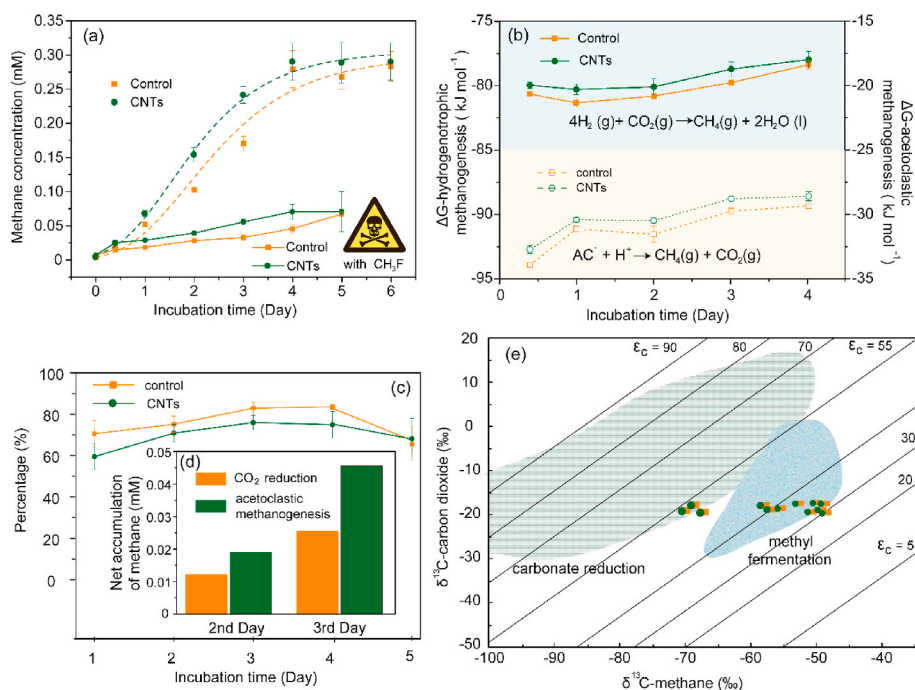


Fig. 4. Methane production in anaerobic soils. Effects of carbon nanotubes (CNTs) on the kinetics of methane production (a). The corresponding ΔG values for CO_2 reduction and direct acetate dismutation (b). Methanogenic pathways revealed by CH_3F inhibition experiments (c) and isotopic fractionation experiments (e). The ratio of methane produced from acetoclastic methanogenesis to the total amount of methane generated based on CH_3F inhibition experiments (d). Background values were obtained from a previous report (Whiticar, 1999). Orange: control; olive: treatments with CNTs. (For interpretation of the references to colour in this figure legend, the reader is referred to the Web version of this article.)

According to equation ($\delta^{13}\text{CH}_4 = f_{ma}\delta_{ma} + (1 - f_{ma})\delta_{mc}$), the percentages of the contribution of the acetoclastic methanogenic pathway to the total methane under the two experimental conditions were approximately $85 \pm 10.18\%$ and $100 \pm 9.29\%$ on the 3rd day. The results of the isotope calculations were basically consistent with the data shown in Fig. 4c. That is, carbon isotopic fractionation experiments show that almost all methane produced with acetate as a direct substrate and CNTs strengthened this pathway in anaerobic soil (Table 1).

3.5. Abundance of bacteria and methanogens responding to carbon nanotubes

The known exoelectrogenic bacteria, such as *Geobacter* and *Shewanella*, did not benefit from the presence of CNTs with a p value of 0.21 (Fig. S3a). Methanosarcinaceae, which is the most metabolically versatile of the methanogenic archaea, had the highest abundance of methanogens in both treatments (Figs. S3b and S4). The abundance of this kind of methanogen in both treatments exceeded 60%. CNTs significantly increased Methanosarcinaceae abundance ($p = 0.00053$), indicating that methane may derive from the decomposition of acetate by Methanosarcinaceae in anaerobic soil.

4. Discussion

4.1. Carbon nanotubes contributed to an increase of acetoclastic methanogenesis in pure culture

This work highlights that CNTs were favorable to both *M. barkeri* and *M. mazei* (Figs. 1 and 2). The culture systems used was pure culture of methanogens. Therefore, there is no DIET process in which electroactive microorganisms generate electrons for methanogens. Very recently, a direct effect of conductive magnetite on pure culture of *Methanosarcina* spp rather than the promotion of DIET was proposed (Fu et al., 2019; Wang et al., 2020). But the study of Fu and colleagues did not show any positive function of CNTs on *M. barkeri*. Combining the experimental results of this study and previous research (Salvador et al., 2017), CNTs accelerating methane production in pure culture of acetotrophic methanogens looks reliable.

In the presence of CH_3F , the slight consumption of acetate caused by

the addition of CNTs may be mainly due to the stronger acetoclastic methanogenesis (Fig. 2a). Based on the author's knowledge of the physiological metabolism of *M. barkeri*, this kind of methanogenic archaea is basically incapable to oxidizing $^{13}\text{CH}_3\text{COOH}$ to produce $^{13}\text{CO}_2$. Reported that a small percentage (2.3%) of $^{13}\text{CH}_3\text{COOH}$ can be converted into $^{13}\text{CO}_2$ through electron bifurcation when providing a high concentration of ferrihydrite. No ferric iron was added in our research, and additional reducing substances, cysteine and Na_2S , were added into the medium. Therefore, it was less likely that methanogenic archaea oxidize acetate through electron bifurcation.

The amount of acetate consumed was approximately 0.01 mmol (Fig. 2a). If the consumed acetate was completely oxidized to CO_2 ($^{13}\text{CH}_3\text{COOH} \rightarrow ^{12}\text{CO}_2 + ^{13}\text{CO}_2$) without the occurrence of acetoclastic methanogenesis, 3% $^{13}\text{CO}_2$ and 3% $^{12}\text{CO}_2$ should be produced with 3% $^{13}\text{CH}_3\text{COOH}$ as the substrate. Therefore, the molar amount of produced $^{13}\text{CO}_2$ was about 3×10^{-7} mol. We determined the value of $^{13}\text{C}/^{12}\text{C}$ of CO_2 in the originally mixed gas, which was approximately 1.088%. Fifteen millilitres of nitrogen and CO_2 mixed gas ($\sim 20\%$ CO_2) was added to the upper space of the anaerobic tube, and the molar amount of $^{12}\text{CO}_2$ was about 1.32×10^{-4} mol. Therefore, the ratio of $^{13}\text{CO}_2/^{12}\text{CO}_2$ should be approximately 0.227%. Additionally, 1 M CO_2 can be converted into 1 M CH_4 . Correspondingly, the ratio of $^{13}\text{CH}_4/^{12}\text{CH}_4$ should be about 0.227% as well. The measured value ($\sim 3\%$) was more than one order of magnitude of the theoretically calculated value. Therefore, this assumption seemed to be untenable (0.227% VS $\sim 3\%$), not to mention that acetate was almost impossible to be completely oxidized without the occurrence of direct acetate dismutation. With 3% $^{13}\text{CH}_3\text{COOH}$ as the substrate, 3% $^{13}\text{CH}_4$ and 3% $^{12}\text{CO}_2$ should be produced through acetoclastic methanogenesis. The measured value was consistent with the theoretically calculated value. Conclusively, CNTs may promote methane production via direct acetate dismutation in the presence of CH_3F .

4.2. Carbon nanotubes stimulated the synthesis of proteins involved in $-\text{COOH}$ oxidation and electron transfer

The synthesis of formylmethanofuran dehydrogenase (Fwd), which is a vital enzyme for the generation of methane via CO_2 reduction (Wagner et al., 2016), was significantly down-regulated (Supplementary

Table 1
Isotopic signatures ($\delta^{13}\text{C}$) of CH_4 and CO_2 produced in the vials.

Treatments	$\delta^{13}\text{C}$ -values of CH_4 (with CH_3F , ‰) ¹	$\delta^{13}\text{C}$ -values of CO_2 (with CH_3F , ‰) ²	α^3	$\delta^{13}\text{C}$ -values of CO_2 (without CH_3F , ‰) ⁴	δ_{inc}^5	δ_{ma}^6	$\delta^{13}\text{C}$ -values of CH_4 (without CH_3F , ‰)	f_{ma} (%)	calculated percent with CH_3F (%)
Control (3rd day)	-67.69 ± 2.29	-19.86 ± 1.13	1.05 ± 0.002	-19.13 ± 0.71	-66.70 ± 1.94	-46.97 ± 0.57	-50.12 ± 2.21	85.00 ± 10.18	82.96
CNTs (3rd day)	-68.46 ± 0.86	-19.16 ± 0.53	1.05 ± 0.001	-17.99 ± 0.05	-67.35 ± 1.16	-50.50 ± 0.35	-50.42 ± 1.47	100.61 ± 9.29	75.98
Control (5th day)	-67.69	-19.86	1.05	-19.66 ± 0.46	-67.49 ± 0.45	-47.59 ± 0.76	-54.58 ± 0.91	64.88 ± 1.47	73.89
CNTs (5th day)	-68.46	-19.16	1.05	-18.48 ± 0.50	-67.82 ± 0.47	-49.65 ± 0.42	-56.20 ± 0.95	63.93 ± 7.66	74.35

¹ $\delta^{13}\text{C}$ -values of CH_4 produced in incubations of slurry in the presence of CH_3F . The $\delta^{13}\text{C}$ values used on the 5th day were the average of those on the 3rd day.

² $\delta^{13}\text{C}$ -values of CO_2 produced in incubations of slurry in the presence of CH_3F . The $\delta^{13}\text{C}$ values used on the 5th day were the average of those on the 3rd day.

³ Calculated with the equation ($\alpha_{\text{CO}_2/\text{CH}_4} = \frac{\delta^{13}\text{C}_{\text{CO}_2} + 1000}{\delta^{13}\text{C}_{\text{CH}_4}(\text{CO}_2) + 1000}$) using $\delta^{13}\text{C}$ -values of CH_4 and CO_2 in the presence of CH_3F .

⁴ $\delta^{13}\text{C}$ -values of CO_2 produced in incubations of slurry without CH_3F .

⁵ Calculated values of $\delta^{13}\text{C}_{\text{CH}_4}$ using (3) and (4) according to the equation shown in (3).

⁶ According to a previous review³⁵, the value of δ_{ma} was calculated by assuming an ϵ of -21% and $\delta_{\text{ma}} = \delta^{13}\text{C}_{\text{soc}+\epsilon}$ at the exhausted condition.

Table 2). Consequently, CNTs did not tend to strengthen the CO_2 reduction pathway. Subdividing the acetate dismutation for methane production, two half-reactions constitute the overall process: electron donating half-reaction and electron accepting half-reaction (Bethke et al., 2011). In the presence of CNTs, the synthesis of proteins involved in the electron donating half-reaction was basically up-regulated (Fig. 3, Table S2). Producing more electrons also requires more electron mediators to participate in transport, such as Fd (Kaster et al., 2011; Yan et al., 2017). However, the electron transfer process is not just Fd's participation. For example, the transfer of electrons in the cell membrane may require methanophenazine (Abken et al., 1998). Under the premise that Fd provides more electrons, CNT-mediated electron transfer may accelerate the entire electron transfer chain.

Some CNTs stuck tightly to the cell surface according to experimental results from transmission electron microscopy (Fig. 5a, c and d). Black nano-scale tubular material can be seen in the field of view. In contrast, no black materials can be found in the control (Fig. 5b). Conductive nano- Fe_3O_4 can replace the structure of cytochromatin-like proteins for transporting electrons (Liu et al., 2015). It is considering that CNTs exerted a function as protein and improved *Methanosarcina* pp. efficiency. Methanogenic archaea tended to reduce the synthesis of proteins involved in the electron accepting half-reaction (Fig. 3, Table S2). With a faster electron supply, the demand for so many enzymes may be reduced. Decreasing the synthesis of protein can also reduce the energy requirement accompanied by the dwindling number of ATPase subunits (Fig. 3).

4.3. Carbon nanotubes benefited methane production independently of electroactive bacteria

In anaerobic soil, CNTs improved the performance of anaerobic systems, and methane production was comparable (Fig. 4a). The function of CNTs to promote methane production in sediment and sludge has been observed in some studies (Li et al., 2015; Zhang et al., 2018). But the proposed explanations were that CNTs promoted electron transfer between the electrogenic bacteria and the methanogens to reduce CO_2 . However, *Geobacter* spp. are the only bacteria demonstrated to participate in DIET with methanogens (Van Steendam et al., 2019). But CNTs did not affect the abundance of *Geobacter* or other canonical electricigens, such as *Shewanella*, in this study.

We also analyzed the electron transfer by means of an electrochemical method. The addition of CNTs did not significantly change the redox peak (Fig. S5), suggesting that the role of CNTs in promoting electron transfer between electromicroorganisms and methanogenic archaea may also be weak. In view of this, the traditional conclusion that conductive materials facilitate DIET between electron-donating bacteria and methanogens to improve CO_2 reduction may not fully explain the phenomenon well (Fig. 5e). It is worth noting that the abundance of methanogenic archaea was improved by CNTs (Figs. S3b and S4). Therefore, CNTs may only benefit methanogenic archaea just as pure cultures.

4.4. Acetoclastic methanogenesis contributed to methane accumulation in anaerobic soils

The inhibitor worked (Fig. 4a), and it was feasible to analyze the contribution of different pathways by inhibiting the acetoclastic methanogenic pathway based on isotopic fractionation (Conrad, 2005). It is widely recognized that the $\delta^{13}\text{C}$ value of methane is more negative when CO_2 is used as a substrate than when methane is obtained using acetate as a precursor (Conrad, 2005). With the application of CH_3F , the $\delta^{13}\text{C}$ -values of methane were very negative and in the range of CO_2 reduction (Conrad and Casper, 2010; Penning et al., 2006). According to Table 1, increased methane production was mainly due to the acetoclastic methanogenesis, which was very consistent with the results shown in Fig. 4e. To the best of our knowledge, this is the first time that

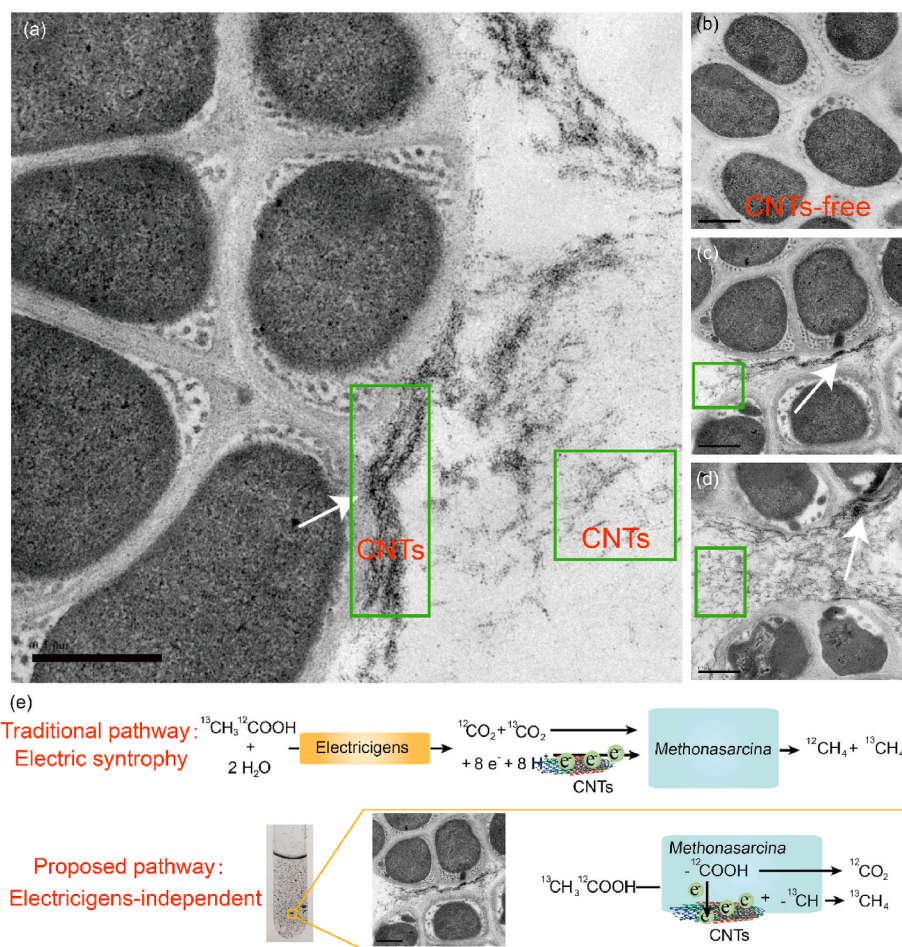


Fig. 5. Surface-associated carbon nanotubes (CNTs) strengthened acetoclastic methanogenesis of *M. barkeri*. Analysis of the distribution of CNTs and cells by transmission electron microscopy (TEM) for the experimental group (a, c and d) and the control (b). The white arrow indicates that the CNTs were in close contact with the cell surface. Linear CNTs can be clearly seen in the green box. The traditional and proposed pathway based on references and findings in this study (e). (For interpretation of the references to colour in this figure legend, the reader is referred to the Web version of this article.)

the capability of carbon nanomaterials to improve direct acetate dismutation has been proposed in natural soil. However, this study used only one kind of soil for verification. To make the conclusion more generalizable, it would be better to verify the promotion of carbon nanomaterials on acetoclastic methanogenesis with different characteristics of soils.

Combined with the energy release of methanogenic archaea, acetoclastic methanogenesis actually releases more energy than CO_2 reduction in a nominal environment (Table S3). The energy, ΔG_A , is the free energy liberated by the group's net reaction. According to the data shown in Table S4, for producing 1 mol of methane, 32 or 1 kJ of energy is available by acetoclastic methanogenesis or hydrogenotrophic methanogenesis, respectively, to *Methanosarcina* (Bethke et al., 2011). Specifically, considering the consumption of ATP during methanogenesis, the useable energy ΔG_u is approximately 21 kJ per mole of methane produced for acetoclastic methanogenesis. However, for hydrogenotrophic methanogenesis, this value is approximately -10 kJ. Thus, the production of 1 mol of methane by this pathway requires an additional source of 10 kJ of energy. Under the premise that CNTs promote both methanogenic pathways (Fig. 4b), energy metabolism may also explain why the proportion of methane production from acetate dismutation was much higher than that from CO_2 reduction in both pure culture and anaerobic soil.

5. Conclusion

In addition to the stimulation of the electric syntrophy between exoelectrogenic bacteria and methanogens by conductive C/Fe-bearing materials, the findings of this study revealed that carbon nanotubes

directly favoured methane production by promoting a route for acetoclastic methanogenesis independently of electrogenic microorganisms. Moreover, with accurate substrates and methanogens, multiple technologies are still needed to analyze the diverse methanogenic processes. More importantly, we not only found this phenomenon with pure culture, but also systematically verified it in environmental samples. Reliable experiments proposed a new model to expand our knowledge of the role of conductive nanomaterials in methanogenic acetate degradation in natural environments.

CRediT authorship contribution statement

Leilei Xiao: Data curation, Formal analysis, Writing - review & editing. **Shiling Zheng:** Writing - review & editing. **Eric Lichtfouse:** Writing - review & editing. **Min Luo:** Writing - review & editing. **Yang Tan:** Writing - review & editing. **Fanghua Liu:** Data curation, Formal analysis.

Declaration of competing interest

The authors declare that they have no competing interests.

Acknowledgments

This research was financially supported by the National Natural Science Foundation of China (no. 41703075, 91751112 and 41573071), the Natural Science Foundation of Shandong Province (no. JQ201608 and ZR2016DQ12) and the Young Taishan Scholars Program of Shandong Province (no. tsqn20161054).

Appendix A. Supplementary data

Supplementary data to this article can be found online at <https://doi.org/10.1016/j.soilbio.2020.107938>.

References

- Abken, H.J., Tietze, M., Brodersen, J., Bumer, S., Beifuss, U., Deppenmeier, U., 1998. Isolation and characterization of methanophenazine and function of phenazines in membrane-bound electron transport of *Methanosarcina mazei* Gol. *Journal of Bacteriology* 180 (8), 2027–2032.
- Bethke, C.M., Sanford, R.A., Kirk, M.F., Jin, Q.S., Flynn, T.M., 2011. The thermodynamic ladder in geomicrobiology. *American Journal of Science* 311 (3), 183–210.
- Conrad, R., 2005. Quantification of methanogenic pathways using stable carbon isotopic signatures: a review and a proposal. *Organic Geochemistry* 36 (5), 739–752.
- Conrad, R., Casper, P., 2010. Stable isotope fractionation during the methanogenic degradation of organic matter in the sediment of an acidic bog lake, Lake Grosse Fuchskuhle. *Limnology & Oceanography* 55 (5), 1932–1942.
- Fu, L., Zhou, T., Wang, J., You, L., Lu, Y., Yu, L., Zhou, S., 2019. Nano-Fe₃O₄ as solid electron shuttles to accelerate acetotrophic methanogenesis by *Methanosarcina barkeri*. *Frontiers in Microbiology* 10, 388.
- Holmes, D.E., Smith, J.A., 2016. Biologically produced methane as a renewable energy source. *Advances in Applied Microbiology* 97, 1–61.
- Hutten, T.J., Bongaerts, H.C.M., Drift, C., Vogels, G.D., 1980. Acetate, methanol and carbon-dioxide as substrates for growth of *Methanosarcina-barkeri*. *Antonie Van Leeuwenhoek Journal of Microbiology* 46 (6), 601–610.
- Ji, Y., Liu, P., Conrad, R., 2018. Response of fermenting bacterial and methanogenic archaeal communities in paddy soil to progressing rice straw degradation. *Soil Biology and Biochemistry* 124, 70–80.
- Kaster, A.K., Moll, J., Parey, K., Thauer, R.K., 2011. Coupling of ferredoxin and heterodisulfide reduction via electron bifurcation in hydrogenotrophic methanogenic archaea. *Proceedings of the National Academy of Sciences of the United States of America* 108 (7), 2981–2986.
- Li, J., Xiao, L., Zheng, S., Zhang, Y., Luo, M., Tong, C., Xu, H., Tan, Y., Liu, J., Wang, O., Liu, F., 2018. A new insight into the strategy for methane production affected by conductive carbon cloth in wetland soil: beneficial to acetoclastic methanogenesis instead of CO₂ reduction. *The Science of the Total Environment* 643, 1024–1030.
- Li, L.L., Tong, Z.H., Fang, C.Y., Chu, J., Yu, H.Q., 2015. Response of anaerobic granular sludge to single-wall carbon nanotube exposure. *Advances in Water Resources* 70, 1–8.
- Li, Q., Li, L., Rejtar, T., Lessner, D., Karger, B., Ferry, J., 2006. Electron transport in the pathway of acetate conversion to methane in the marine archaeon *Methanosarcina acetivorans*. *Journal of Bacteriology* 88 (2), 702–710.
- Liu, F., Rotaru, A.E., Shrestha, P.M., Malvankar, N.S., Nevin, K.P., Lovley, D.R., 2012. Promoting direct interspecies electron transfer with activated carbon. *Energy & Environmental Science* 5 (10), 8982.
- Liu, F.H., Rotaru, A.E., Shrestha, P.M., Malvankar, N.S., Nevin, K.P., Lovley, D.R., 2015. Magnetite compensates for the lack of a pilin-associated c-type cytochrome in extracellular electron exchange. *Environmental Microbiology* 17 (3), 648–655.
- Liu, P.F., Klose, M., Conrad, R., 2018. Temperature effects on structure and function of the methanogenic microbial communities in two paddy soils and one desert soil. *Soil Biology and Biochemistry* 124, 236–244.
- Lu, J., Chang, J., Lee, D., 2020. Adding carbon-based materials on anaerobic digestion performance: a mini-review. *Bioresour. Technology* 300, 122696.
- Martins, G., Salvador, A.F., Pereira, L., Alves, M.M., 2018. Methane production and conductive materials: a critical review. *Environmental Science and Technology* 52 (18), 10241–10253.
- Morita, M., Malvankar, N.S., Franks, A.E., Summers, Z.M., Giloteaux, L., Rotaru, A.E., Rotaru, C., Lovley, D.R., 2011. Potential for direct interspecies electron transfer in methanogenic wastewater digester aggregates. *mBio* 2, e00159-11.
- Penning, H., Claus, P., Casper, P., Conrad, R., 2006. Carbon isotope fractionation during acetoclastic methanogenesis by *Methanosarcina concilii* in culture and a lake sediment. *Applied and Environmental Microbiology* 72 (8), 5648–5652.
- Rai, P.K., Kumar, V., Lee, S., Raza, N., Kim, K.H., Ok, Y.S., Tsang, D.C.W., 2018. Nanoparticle-plant interaction: implications in energy, environment, and agriculture. *Environment International* 119, 1–19.
- Rother, M., Metcalf, W., 2004. Anaerobic growth of *Methanosarcina acetivorans* C2A on carbon monoxide: an unusual way of life for a methanogenic archaeon. *Proceedings of the National Academy of Sciences of the United States of America* 101 (48), 16929–16934.
- Salvador, A.F., Martins, G., Melle-Franco, M., Serpa, R., Stams, A.J.M., Cavaleiro, A.J., Pereira, M.A., Alves, M.M., 2017. Carbon nanotubes accelerate methane production in pure cultures of methanogens and in a syntrophic coculture. *Environmental Microbiology* 19 (7), 2727–2739.
- Song, X., Liu, J., Jiang, Q., Zhang, P., Shao, Y., He, W., Feng, Y., 2019. Enhanced electron transfer and methane production from low-strength wastewater using a new granular activated carbon modified with nano-Fe₃O₄. *Chemical Engineering Journal* 374, 1344–1352.
- Stumm, W., Morgan, J.J., 1996. *Aquatic Chemistry: Chemical Equilibria and Rates in Natural Waters*. John Wiley & Sons, Inc., Hoboken.
- Usman, M., Farooq, M., Wakeel, A., Nawaz, A., Cheema, S.A., Rehman, H.U., Ashraf, I., Sanaullah, M., 2020. Nanotechnology in agriculture: current status, challenges and future opportunities. *The Science of the Total Environment* 721, 137778.
- Van Steendam, C., Smets, I., Skerlos, S., Raskin, L., 2019. Improving anaerobic digestion via direct interspecies electron transfer requires development of suitable characterization methods. *Current Opinion in Biotechnology* 57, 183–190.
- Viggi, C.C., Rossetti, S., Fazi, S., Paiano, P., Majone, M., Aulenta, F., 2014. Magnetite particles triggering a faster and more robust syntrophic pathway of methanogenic propionate degradation. *Environmental Science and Technology* 48 (13), 7536–7543.
- Wagner, T., Ermler, U., Shima, S., 2016. The methanogenic CO₂ reducing-and-fixing enzyme is bifunctional and contains 46 [4Fe-4S] clusters. *Science* 354 (6308), 114–117.
- Wang, H., Byrne, J.M., Liu, P.F., Liu, J., Dong, X.Z., Lu, Y.H., 2020. Redox cycling of Fe (II) and Fe (III) in magnetite accelerates acetoclastic methanogenesis by *Methanosarcina mazei*. *Environmental Microbiology Reports* 12, 97–109.
- Whiticar, M., 1999. Carbon and hydrogen isotope systematics of bacterial formation and oxidation of methane. *Chemical Geology* 161, 291–314.
- Xiao, L., Liu, F., Lichtfouse, E., Zhang, P., Feng, D., Li, F., 2020. Methane Production by Acetate Dismutation Stimulated by *Shewanella oneidensis* and carbon materials: as an alternative to classical CO₂ reduction. *Chemical Engineering Journal* 389, 124469.
- Xiao, L., Liu, F., Liu, J., Li, J., Zhang, Y., Yu, J., Wang, O., 2018. Nano-Fe₃O₄ particles accelerating electromethanogenesis on an hour-long timescale in wetland soil. *Environmental Sciences: Nano* 5 (2), 436–445.
- Xiao, L., Liu, F., Xu, H., Feng, D., Liu, J., Han, G., 2019. Biochar promotes methane production at high acetate concentrations in anaerobic soils. *Environmental Chemistry Letters* 17, 1347–1352.
- Xiao, L., Sun, R., Zhang, P., Zheng, S., Tan, Y., Li, J., Zhang, Y., Liu, F., 2019. Simultaneous intensification of direct acetate cleavage and CO₂ reduction to generate methane by bioaugmentation and increased electron transfer. *Chemical Engineering Journal* 378, 122229.
- Xiao, L., Wei, W., Luo, M., Xu, H., Feng, D., Yu, J., Huang, J., Liu, F., 2019. A potential contribution of a Fe(III)-rich red clay horizon to methane release: biogenetic magnetite-mediated methanogenesis. *Catena* 181, 104081.
- Xiao, L., Xie, B., Liu, J., Zhang, H., Han, G., Wang, O., Liu, F., 2017. Stimulation of long-term ammonium nitrogen deposition on methanogenesis by Methanocellaceae in a coastal wetland. *The Science of the Total Environment* 595, 337–343.
- Yan, Z., Wang, M.Y., Ferry, J.G., 2017. A ferredoxin-and F₄₂₀H₂-dependent, electron-bifurcating, heterodisulfide reductase with homologs in the domains bacteria and archaea. *mBio* 8 (1), e02285-16.
- Zehnder, A.J.B., Wuhrmann, K., 1977. Physiology of a methanobacterium strain az. *Archives of Microbiology* 111 (3), 199–205.
- Zhang, W., Zhang, J.C., Lu, Y.H., 2018. Stimulation of carbon nanomaterials on syntrophic oxidation of butyrate in sediment enrichments and a defined coculture. *Scientific Reports* 8, 12185.
- Zhu, Z.K., Ge, T.D., Liu, S.L., Hu, Y.J., Ye, R.Z., Xiao, M.L., Tong, C.L., Kuzyakov, Y., Wu, J.S., 2018. Rice rhizodeposits affect organic matter priming in paddy soil: the role of N fertilization and plant growth for enzyme activities, CO₂ and CH₄ emissions. *Soil Biology and Biochemistry* 116, 369–377.

Supplementary material

Carbon nanotubes accelerate acetoclastic methanogenesis: From pure cultures to anaerobic soils

Preparation of anaerobic slurry

The bottles were flushed with N₂ for approximately 30 min and incubated statically at 30°C in a dark room. After five weeks of incubation, the incubated soil reached a high methane production potential with a methane concentration of about 100,000 ppm. Then, the incubated soil (5 mL) was dispensed into sterile 11-mL serum vials, which were pre-evacuated, flushed with high-purity N₂, and incubated statically at 30 C.

Samples Preparation and TMT Labeling

Samples of methanogens were lysed by using lysis buffer (300 µL) supplemented with 1 mM PMSF and sonicated for 3 min. After centrifugation of 15 min (15000 g), we collected the supernatant. Bradford assay was used to test protein concentration and protein was aliquoted to store at -80°C. For each sample, 100 µg of proteins were mixed with 120 µL reducing buffer (10 mM DTT, 8 M Urea, 100 mM TEAB, pH 8.0) in Amicon® Ultra-0.5 Centrifugal Filter (10 kDa) and incubated at 60°C for 60 min. Then iodoacetamide was added to the solution with the final concentration of 50 mM and incubated for 40 min at room temperature in the dark. After centrifugation at 12000 rpm for 20 min, samples were washed three times with triethylammonium bicarbonate buffer (TEAB) and digested with trypsin (Promega, Madison, WI, USA) (enzyme to protein ratio 1:50) at 37°C overnight. Digested peptides were labeled with TMT reagents (Thermo Fisher Scientific) according to the manufacturer's instructions. For each 6-plex TMT, control samples were labeled with TMT tags 126, 127, 128 and treatments with CNTs were labeled with TMT tags 129, 130, and 131, respectively. Equal amounts of TMT-labeled peptides were mixed and dried, then resuspended in buffer A (2% acetonitrile, 98% water with ammonia at pH 10) and fractionated by 1100 HPLC System (Agilent).

Proteomic Analysis by LC-MS/MS

Peptides were redissolved with 0.1% formic acid (FA) and analyzed on a Q-Exactive mass spectrometer (Thermo Fisher Scientific, Waltham, MA, USA) coupled with a nanospray Flex source (Thermo, USA). Samples were loaded and separated by a C18 column (15 cm × 75 µm) on an EASY - nLC™ 1200 system (Thermo, USA) in Qingdao OeBiotech. Co., Ltd. The flow rate was 300 nL/min and linear gradient was 90 min. The mass spectrometer was operated in the data-dependent mode with positive polarity at electrospray voltage of 2 kV. Full scan MS spectra (m/z 300–1600) were acquired in the orbitrap with the resolution as 70 K, the automatic gain control (AGC) target was 1e6 and the maximum injection time was 80 ms. The top 10 intense ions were isolated for HCD MS/MS fragmentation. In MS2, the resolution was 17500 and the AGC target was 2e5. Fragmentation was performed with normalized collision energy (NCE) of 32% and dynamic exclusion duration of 15 s.

Mass spectrometry data analysis

The mass spectrometry (MS) raw data were analyzed with Proteome Discoverer software (version 2.2) using the Sequest search engine to search against the *Methanosarcina barkeri* database (UniProtKB, release 2019_03). The following parameters were applied: precursor mass tolerance was 20 ppm; fragment tolerance was 0.5 Da; the dynamic modifications were oxidation (M); the static modification was carbamidomethyl (C) and TMT labeling of amines and lysine; a maximum of two missed cleavages were allowed. Peptides with FDR < 0.01 (based on the target-decoy database algorithm) were used for protein grouping. Protein groups identified ≥ 1 peptides were considered for further analysis and only unique peptides were used for protein quantification. The mass spectrometry raw data were deposited to the iProX (<http://iprox.org>). URL: <https://www.iprox.org/page/PSV023.html?url=1555463853480QxPM>, Password: CO2T

By analyzing the clustering results, based on the credible data in the results, the fold change value was obtained by dividing the average value of the CNTs group data by the average value of the control group data, and the *p*-value of each group was calculated. It was considered that *p*-value less than or equal to 0.05 was regarded as a differential protein. Cluster Profiler package in R language was used to analyze differential proteins, enrichKEGG function was used to compare differential proteins data in KEGG database, and DOTPLOT was used to map the results of signal pathway comparison. With *p*-value equal to 0.05 as the standard, we used cnetplot function to map the change relationship between genes and signaling pathways based on the data with significant difference in change, in which the color difference

was fold change value.

Electrochemical measurements

A single-chamber three-electrode electrochemical cell was used to conduct CV measurements for characterizing the electron transfer rate. Three electrodes were reference electrode (Ag/AgCl), graphite plate electrode (3.0 cm × 2.5 cm × 0.3 cm, working electrode), and platinum electrode (counter electrode). Incubated soil (~ 70 mL) was poured into the electrochemical cell. CNTs concentration was 0.2g/L as well. CVs were measured using an electrochemical workstation (CHI660e, Chenhua, China). The working electrode had a scan voltage between -1.2 and 1.2 V (versus Ag/AgCl), and the scan rates were 40 –140 mV/s.

Table 1 Proteins tested by proteome may be involved in acetoclastic methanogenesis.

Gene Name	Shorthand in Figure 3	Abundance for control			Abundance for treatment with CNTs		<i>p</i> value	
		C1	C2	C3	T1	T3		
ackA	ackA	93	96.9	97.1	102.7	100.8	4.69*10 ⁻⁰²	
Mbar_A1136	At1	106.1	117.7	114.5	81.6	80	5.76*10 ⁻⁰³	
Mbar_A2520	At2	69.2	68.3	68.9	131.1	128.6	9.46*10 ⁻⁰⁶	
Mbar_A3525	Codh-Acs1	87	92.9	88.9	116.2	114.7	1.54*10 ⁻⁰³	
Mbar_A3717	Codh-Acs2	65.1	66.7	68	135.1	136	9.79*10 ⁻⁰⁶	
Mbar_A0640	HdrC	88.9	111	95.4	101.9	103.1	6.64*10 ⁻⁰¹	
Mbar_A0639	HdrB	91.5	89.4	90	107.4	107.9	2.37*10 ⁻⁰⁴	
Mbar_A1952	HdrA1	116.8	118.3	118.8	83.4	84.5	3.78*10 ⁻⁰⁵	
Mbar_A2589	HdrA2	107.5	106.4	106.9	93.5	94.3	1.29*10 ⁻⁰⁴	
hdrD	HdrD	112.9	116.9	111.9	79.5	68.6	3.07*10 ⁻⁰³	
mtrA	mtrA	105.1	100.7	102.4	96.3	96.1	2.90*10 ⁻⁰²	
mtrB	mtrB	104.8	101.8	104.1	102.5	103.5	6.76*10 ⁻⁰¹	
mtrD	mtrD	117.7	111.2	115.7	84.3	86.8	1.58*10 ⁻⁰³	
mtrE	mtrE	122.5	117.3	120.7	79.4	79	2.45*10 ⁻⁰⁴	
mtrF	mtrF	93.2	101.7	100.8	100.5	97.9	8.72*10 ⁻⁰¹	
mtrG	mtrG	125.9	121.4	122.4	74.7	74.9	1.06*10 ⁻⁰⁴	
mtrH	mtrH	108.7	103.9	106.7	94.4	94.4	6.80*10 ⁻⁰³	
mcrA	mcrA	100.1	102.5	100.8	94.8	96.3	1.39*10 ⁻⁰²	
mcrB	mcrB	111.5	114.7	112.9	84.4	83.7	1.65*10 ⁻⁰⁴	
mcrC	mcrC	75.2	75.2	77	122.3	125.8	6.83*10 ⁻⁰⁵	
mcrD	mcrD	98.7	98.9	100.4	97.2	102.7	7.94*10 ⁻⁰¹	
mcrG	mcrG	99.6	102.3	100.8	93.3	94.1	6.37*10 ⁻⁰³	
atpA	atpA	121.3	119.4	121.2	77.3	79.3	3.77*10 ⁻⁰⁵	
atpB	atpB	137	136.2	137.4	61.8	63.8	3.62*10 ⁻⁰⁶	
atpC	atpC	114.6	114.6	113.4	85.9	87.9	8.05*10 ⁻⁰⁵	
atpD	atpD	128.1	125.1	128.3	73.3	73.5	3.39*10 ⁻⁰⁵	
atpE	atpE	137.3	127	130.7	68.3	69.8	5.37*10 ⁻⁰⁴	
atpF	atpF	98.5	94.3	94.8	112.7	109.4	5.55*10 ⁻⁰³	
atpI	atpI	127.7	123.4	125.8	74.2	75.4	7.75*10 ⁻⁰⁵	
Mbar_A3421	Fd1	78.4	78	73.2	127.2	131.4	2.81*10 ⁻⁰⁴	
Mbar_A2086	Fd2	76.3	72.6	72.5	121	117.6	2.01*10 ⁻⁰⁴	
Mbar_A0148	EchE	129.9	130.8	130.4	68.4	68.1	4.09*10 ⁻⁰⁷	
Mbar_A0149	EchD	88.7	93	94	97.9	99.3	5.34*10 ⁻⁰²	
Mbar_A0150	EchC	113	101.8	107.6	104.8	106.5	6.96*10 ⁻⁰¹	
Mbar_A0147	EchF	124.4	121.8	122.4	77.7	79	3.55*10 ⁻⁰⁵	
frhA	frhA	99.2	109.4	102.2	92.2	92.3	6.23*10 ⁻⁰²	
frhB	frhB	106	102.8	107.4	95.2	98	2.31*10 ⁻⁰²	
frt	frt	103.8	100.2	102.3	100.6	101.9	5.95*10 ⁻⁰¹	
fmdC	fmdC	109.2	105.6	108.1	96.3	96.7	4.00*10 ⁻⁰³	
Mbar_A0795	fwdE1	94.6	94.6	98	107.6	113.1	1.02*10 ⁻⁰²	
Mbar_A1291	fwdD	104.1	109.7	108.7	94.7	97.1	1.69*10 ⁻⁰²	
Mbar_A1287	fwdE2	121.6	113.9	113.3	87.1	87.6	3.58*10 ⁻⁰³	
Mbar_A1763	fwdB2	109.8	104.8	106.4	94.8	96.6	1.13*10 ⁻⁰²	
Mbar_A1292	fwdB	104.2	96.4	102.3	103.5	97	8.66*10 ⁻⁰¹	

Table 2 Kinetic parameters of the methane production by fitting the modified Gompertz equation.

Treatment	Measured value*	Kinetic model parameters			
		λ (Day)	R_{\max} (mM D ⁻¹)	P_{\max} (mM)	R^2
control	0.282±0.022	0.629 ±0.223	0.087±0.014	0.297 ±0.016	0.999
CNT	0.289±0.027	0.426 ±0.137	0.102±0.010	0.304±0.011	0.999

*Measured maximum concentration of methane at the end of the batch experiments (mM)

Table 3 Electron accepting and donating processes of methane production as defined by free energy change in a nominal anoxic geochemical environment^a

Half-reactions	Metabolic pathways	Equation	ΔG (kJ mol ⁻¹)
Electron donating half-reactions	acetotrophy	$CH_3COO^- + 4H_2O \rightarrow 2HCO_3^- + 9H^+ + 8e^-$	-216
	hydrogentrophy	$4H_2(aq) \rightarrow 8H^+ + 8e^-$	-185
Electron accepting half-reaction	methanogenesis	$HCO_3^- + 9H^+ + 8e^- \rightarrow CH_4 + 3H_2O$	184

^a Related data refer to Bethke et al.⁵. 25 °C; pH 7; 1 mmol kg⁻¹ Ca²⁺, CO₂(aq) + HCO₃⁻, SO₄²⁻, NO³⁻, Fe²⁺, and Mn²⁺; 1 μmol kg⁻¹ CH₃COO⁻, CH₄(aq), HS⁻, and NH₄⁺; 1 nmol kg⁻¹ H₂(aq); N₂(aq) at atmospheric saturation.

Table 4 Net reactions for two major methanogenesis, the reactions' available (ΔG_A) and usable energies (ΔG_U) in a nominal geochemical environment^a

Metabolic pathways	Equation	ΔG_A (kJ mol ⁻¹)	ΔG_U (kJ mol ⁻¹)
Acetoclastic methanogenesis	$CH_3COO^- + H_2O \rightarrow CH_4(aq) + HCO_3^-$	32	21
Hydrogenotrophic methanogenesis	$4H_2(aq) + HCO_3^- + H^+ \rightarrow CH_4(aq) + 3H_2O$	1	-10

^a Environmental conditions are defined the in footnote to Table 3 and refers to Bethke et al.⁵.

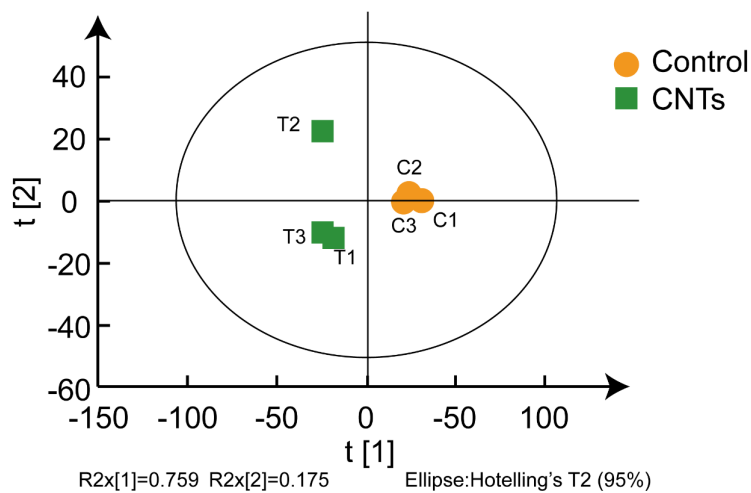


Figure S1 Principal component analysis of proteome samples. C1, C2 and C3 were three replicates of the control group. T1, T2 and T3 were three replicates of the carbon nanotubes (CNTs) group. This results showed that the sample 2, T2, was an abnormal sample, which was not in the scope of subsequent analysis.

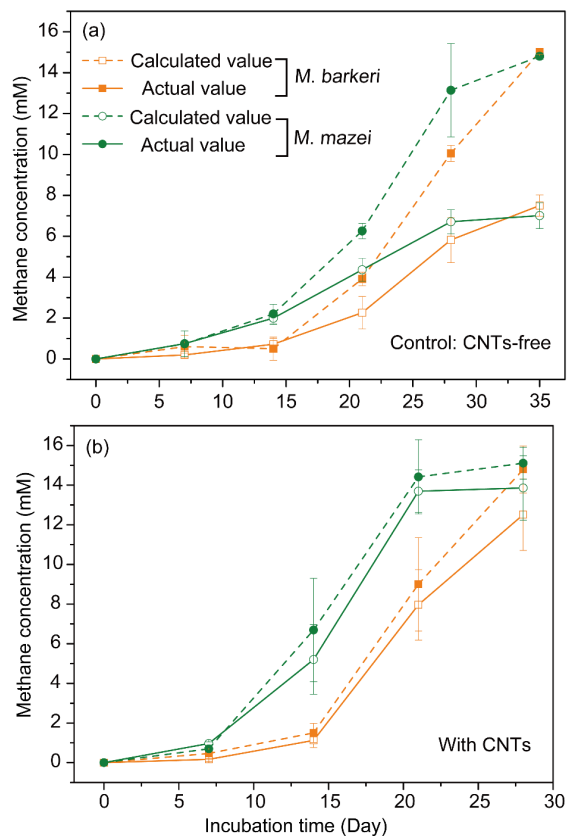


Figure S2 Calculated and actual methane concentrations in pure cultures. The calculated methane is based on the equation: $\text{CH}_3\text{COO}^- + \text{H}^+ \rightarrow \text{CH}_4 + \text{CO}_2$. According to the consumption of acetate, we calculated the methane produced in theory.

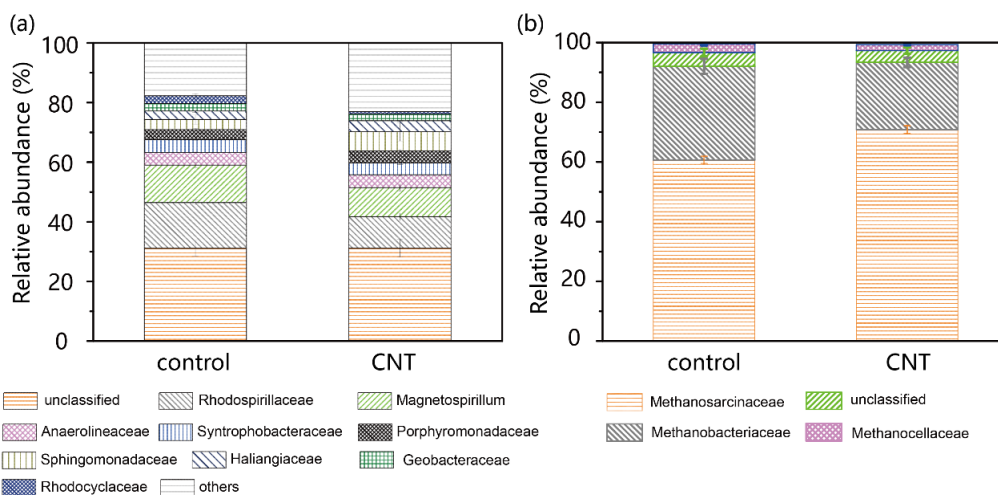


Figure S3. Communities of bacteria (a) and methanogenic archaea (b) at the family level in anaerobic soils after 6 days incubation. Relative abundances of less than 0.8%, for bacteria, and 1.9%, for methanogenic archaea, were classified into the group. 'others'.

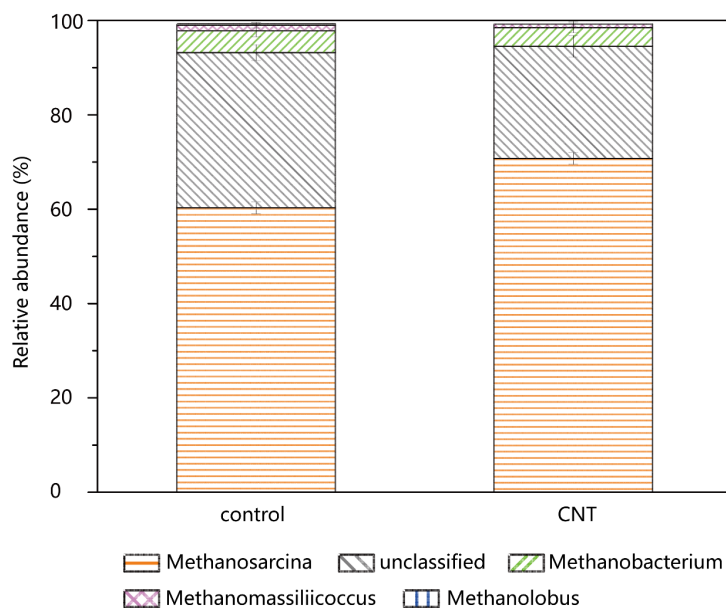


Figure S4. Community of methanogenic archaea at the genus level in incubated soil.

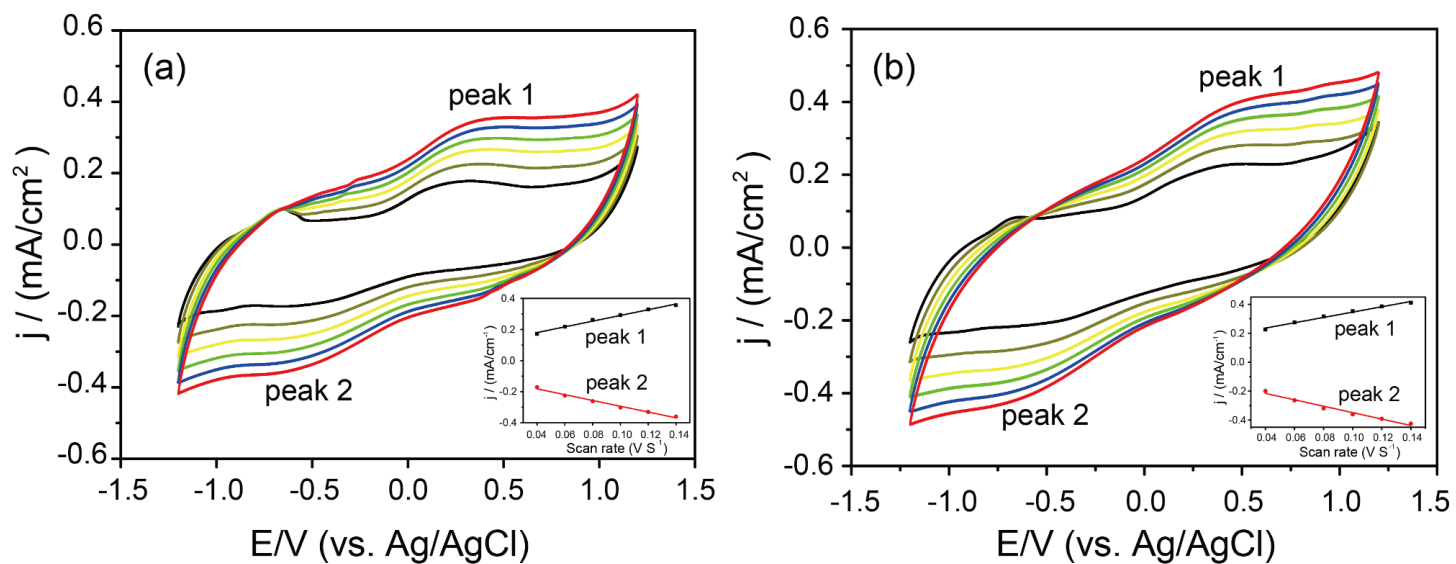


Figure S5 Cyclic voltammetry at different scan rates of 40, 60, 80, 100, 120, and 140 mV s⁻¹ (from the inner to outer) for unamended treatment (a) and treatment with carbon nanotubes (CNTs) (b). (Insets) Peak currents are presented as a function of scan rates.